Article

AMERICAN ORTHOPAEDIC FOOT & ANKLE SOCIETY

Foot & Ankle International®
1–7

DOI: 10.1177/10711007241309915
journals.sagepub.com/home/fai

Talar Morphology of Charcot-Marie-Tooth Patients With Cavovarus Feet

Andrew C. Peterson, MS[1], Melissa R. Requist, BS[1], Jacob C. Benna, BS[1,2], Jayson R. Nelson, BS[1], Shireen Elhabian, MSc, PhD[3], Cesar de Cesar Netto, MD, PhD[4], Timothy C. Beals, MD[5], and Amy L. Lenz, PhD[1,6]

Abstract

Background: Charcot-Marie-Tooth disease (CMT), a common inherited neurologic disorder, significantly impacts the morphology of foot bones, particularly the talus. The disease has been classified into types based on specific mutations, with the most common being CMT type 1 (CMT1; demyelinating) and CMT type 2 (CMT2; axonal). However, the specific osseous morphologic variations in CMT patients and their major genetic subgroups remain insufficiently understood, posing challenges in clinical management and surgical intervention.

Methods: This study analyzed talar morphology in individuals with CMT compared with a healthy control group, employing a single-bone statistical shape model and talar neck offset angle measurements. Participants included 18 CMT individuals (yielding 29 tali) and 43 healthy controls. For individuals with CMT, the average age at diagnosis was 36.5 ± 19.8 years, with a mean interval of 8.6 years between diagnosis and imaging. Talar morphology was evaluated using weightbearing computed tomography and subsequent morphologic and angular analysis.

Results: Differences were observed in talar morphology between CMT and healthy individuals. Notably, CMT1 and CMT2 tali exhibited a flatter talar dome and more medial talar head and neck compared with controls. Additionally, the CMT1 and CMT2 subgroups both had a more medially oriented talar neck based on the talar neck offset angle compared with the controls.

Conclusion: The findings illustrate significant morphologic variations in the talus of CMT patients, indicating the need for type-specific clinical approaches in treating CMT-related foot deformities. Understanding these talar variations is crucial for tailoring surgical techniques and orthotic designs, and developing effective rehabilitation protocols for individuals with CMT, potentially improving patient care and outcomes.

Level of Evidence: Level III, retrospective case control study.

Keywords: Charcot-Marie-Tooth disease, talar morphology, statistical shape modeling, talar neck offset angle, foot and ankle biomechanics

Introduction

Charcot-Marie-Tooth disease (CMT) is the most commonly inherited neurologic disorder, affecting approximately 1 in 2500 individuals, affecting their quality of life.[13,17] The disease can be classified into types based on specific mutations, with the most common being CMT type 1 (CMT1; demyelinating) and CMT type 2 (CMT2; axonal).[3,21] The progression of CMT affects both sensory and motor nerves in the limbs, particularly in the legs and feet, resulting in selective muscle weakness and atrophy. This can lead to imbalance between agonist and antagonist musculature and progressive deformities of the foot and ankle, most

[1]Department of Orthopaedics, University of Utah, Salt Lake City, UT, USA
[2]Reno School of Medicine, University of Nevada, Reno, NV, USA
[3]School of Computing, University of Utah, Salt Lake City, UT, USA
[4]Department of Orthopaedic Surgery, University of Duke, Durham, NC, USA
[5]The Orthopedic Partners, Park City, UT, USA
[6]Department of Biomedical Engineering, University of Utah, Salt Lake City, UT, USA

Corresponding Author:
Amy L. Lenz, PhD, Department of Orthopaedics and Biomedical Engineering, University of Utah, 590 Wakara Way, Salt Lake City, UT 84108, USA.
Email: amy.lenz@utah.edu

commonly equinus cavovarus and adductus deformity, with associated balance and gait disorders.[9] Studies have suggested that these alignment abnormalities in CMT may reflect underlying dysmorphic bone dimensions, rather than solely imbalanced soft tissue forces, as seen in idiopathic cavovarus deformities.[4] Although other work has delineated the neurologic progression and the consequential soft tissue alterations in the foot and ankle of individuals with CMT,[7,19] there remains a gap in the comprehensive understanding of osseous morphologic variations within this population.[11] Addressing this gap regarding osseous morphology between types of CMT and healthy individuals may influence treatment and surgical techniques and emphasize the need for tailored procedures.

Given the multifaceted and complex nature of this disease, this study focused on analyzing the talar morphology in the context of CMT. The talus is integral to various movements of the foot and is responsible for transmitting forces from the foot to the leg.[14] Its unique anatomical position, coupled with significant articular surface coverage, highlights the importance of a detailed understanding of its morphology for clinical management and potential surgical interventions.[6] Additionally, the orientation of talar articular surfaces dictates the relative positions and movements of adjacent bones such as the tibia, navicular, and calcaneus, directly influencing the overall function of the foot and ankle. Clarifying these variations is valuable when defining interventions that accommodate the mechanical demands placed on the feet of patients with CMT.

Therefore, in this study, we aimed to quantify talar morphologic variation between types of CMT and healthy individuals. We hypothesize that the talar neck in both CMT types will exhibit increased medial angulation than those observed in healthy individuals. This analysis aimed to advance our understanding of the impact that the motor imbalance in CMT disease has on the development of talar morphology. This may inform our understanding of pathologic kinematics of hindfoot function, which can lead to more tailored operative and nonoperative treatments for CMT patients to improve patient care and outcomes.

Materials and Methods

Participant Recruitment and Screening

Following institutional review board (IRB) approval, we retrospectively assessed weightbearing computed tomography (WBCT) scans of tali from individuals with a clinical cavovarus foot deformity secondary to CMT as well as healthy controls. The CMT group consisted of 29 tali from 18 individuals (average age at scan: 45.1 ± 20.8 years; average at diagnosis: 36.5 ± 19.8 years; average time between diagnosis and imaging: 8.6 years; 7 female patients). Type diagnoses divided our CMT group into 18 tali from 10 individuals with CMT1 (average age at scan: 45.8 ± 19.3 years; average at diagnosis: 33.4 ± 15.9 years) and 11 tali from 8 individuals with CMT2 (average age at scan: 43.8 ± 23.9 years; average at diagnosis: 41.5 ± 24.9 years). Although the sample sizes for these subgroups are limited and include bilateral scans, the rarity of CMT in the general population restricts the feasibility of large-scale 3D analyses, as noted in similar studies on comparable populations.[11,12,16,20] No individuals had foot or ankle surgery before the scan, and all individuals with CMT had type confirmed via genetic testing and only those with type 1 or type 2 were included. The healthy control group consisted of 43 tali from 43 individuals (age: 41.69 ± 8.82 years; 28 female patients) and were screened to have a rectus hindfoot with typical midfoot and hindfoot alignment.

Image Acquisition and Model Preparation

All individuals had WBCT scans (CurveBeam PedCAT; 0.37-mm^3 voxel size). The scans were automatically segmented using dedicated software (Paragon 28, Disior, Bonelogic Ortho Foot and Ankle v2.1.1, Helsinki, Finland), manually verified in Mimics (Mimics v24.0; Materialise), and consistently decimated and smoothed in 3-matic (3-matic v16.0; Materialise) to ensure anatomical accuracy. Left-sided models were mirrored to right-sided models for uniform analysis, and all tali were aligned using an iterative closest point algorithm in MATLAB (R2023a; MathWorks, Natick, MA) in preparation for morphologic analysis.[22]

Morphology Analysis: Statistical Shape Modeling

To analyze variations in talar morphology, we generated an SSM of the talus using open-source software (ShapeWorks v6.3.2, University of Utah; www.shapeworks.sci.utah.edu). This software compares bone shapes by placing corresponding points (or particles) consistently across each bone model.[5] Each talus was represented with 1,024 particles, and a Procrustes analysis was applied to remove differences in size, allowing us to focus solely on shape variations.

We used principal components analysis (PCA), a method that identifies major patterns (or modes) of shape variation across the cohort.[8] To determine which patterns were most relevant, we applied a parallel analysis algorithm, which is a statistical approach for selecting meaningful modes of variation to retain in the analysis.[10]

We then tested differences in these shape patterns between groups. For normal data, an analysis of variance was used and for non-normal data, a Kruskal-Wallis test was used. Post hoc comparisons were adjusted with a Holm-Sidak correction, and significance was set at $\alpha = 0.05$. Finally, we calculated surface distances to visually compare differences between each group's average shape and the

variations seen at 2 SDs from the mean and between the mean shapes of each group.

Morphology Analysis: Talar Neck Offset Angle

To analyze the orientation of the talar neck with respect to the talar body, the talar neck offset angle (TNOA) was calculated on each talus using open-source software in MATLAB.[15] The toolbox automatically and mathematically calculates anatomical coordinate systems (ACS) based on the unique contours of each bone, ensuring precise orientation measurements.[15] The ACSs corresponding to the tibiotalar and talonavicular joints were for their alignment with key anatomical landmarks—the talar trochlear facets and the talar neck, respectively. The anterior-posterior (AP) vectors from these 2 ACSs served as the basis for our TNOA calculations in MATLAB (Figure 1). A 2-sample *t* test was used to compare the angles between groups with an alpha level set at 0.05.

To quantify the effect size, we calculated a Cohen *d* value between the healthy and CMT groups.

Results

Morphology Analysis: Statistical Shape Modeling

A parallel analysis of the SSM yielded 9 PCA modes of variation to retain, accounting for 74.8% of the explained variance. The shape variations for each of the 9 modes are described in Table 1. Of those 9 modes, 2 PCA modes presented significant differences between groups. In the first PCA mode, the healthy group differed significantly from the CMT1 ($p < 0.0001$) and CMT2 ($P = .0027$) groups, with the healthy group showing a more curved talar dome and an inferior-lateral talar head and neck position, while the CMT groups exhibited a flatter dome with a superior-medial talar head and neck position (Figure 2). In the third PCA mode, the CMT2 group differed significantly from the healthy ($P = .0432$) and CMT1 ($P = .0281$) groups, with the healthy and CMT1 groups showing a trend toward a smaller posterior process and a posterior-positioned talar dome, whereas the CMT2 group exhibited a more anterior dome and a larger posterior process (Figure 3).

The mean shapes for the 3 groups were also computed to assess morphologic variations (Figure 4). Comparing the mean shapes of the CMT1 and CMT2 groups to the healthy group, we observed trends paralleling the shape score distributions. Specifically, the CMT groups exhibited a flatter talar dome and more medial talar head and neck compared with the healthy group.

Morphology Analysis: Talar Neck Offset Angle

The TNOA analysis revealed statistically significant differences between certain groups, whereas others did not show significant variation (Table 2). The healthy control group exhibited an average TNOA of 26.85 ± 2.03 degrees. The CMT1 type had an average TNOA of 28.22 ± 2.05 degrees and the CMT2 type had an average TNOA of 29.60 ± 3.31 degrees (Figure 5). Statistical analysis revealed significant differences between healthy and CMT1 ($P = .0201$) and healthy and CMT2 ($P = .0010$), but not significant differences between CMT1 and CMT2 ($P = .1742$). The Cohen *d* calculation had a large effect size ($d = 0.8043$).

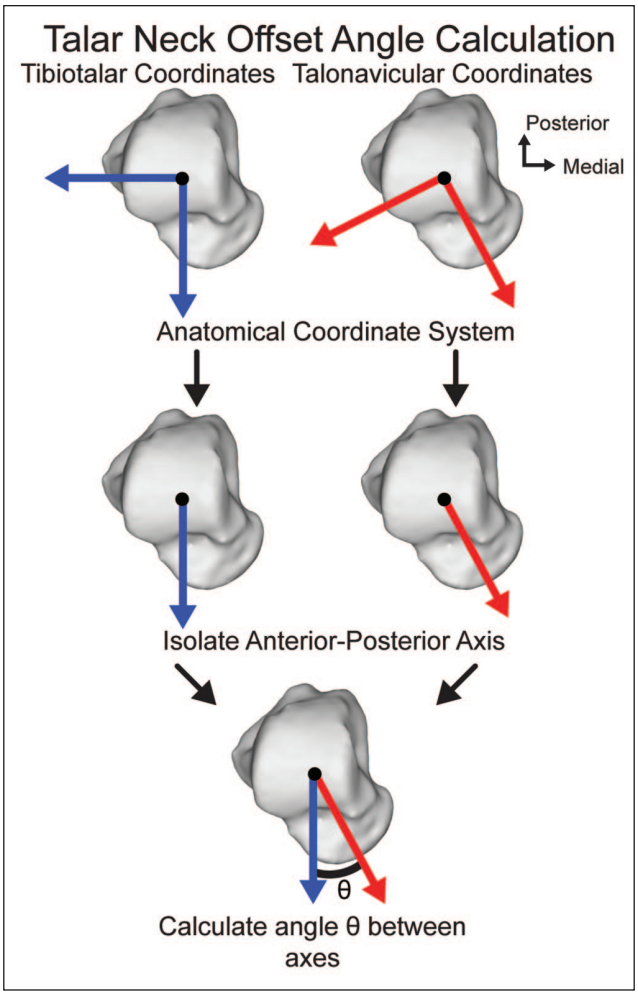

Figure 1. Methodology of 3D talar neck offset angle calculation from the Automatic Anatomical Foot and Ankle Toolbox.

Discussion

In this study, we aimed to quantify morphologic variation in the talus among cavovarus deformity patients with different types of CMT compared with a healthy control group using SSM and TNOA measurements. Our findings revealed a consistent pattern across the cavovarus CMT spectrum, with the talar dome exhibiting a flatter profile and the talar

Table 1. Talar Modes of Variation With Explained Variance and Qualitative Explanation of Primary Morphologic Variations Across the SDs of That Mode.

Talus Mode	Variance, %	Morphology Variations From −2 SD to +2 SD
1[a]	25.3	Talar dome flattens; talar neck angulates superior-medially
2	13.8	Medial talar trochlear facets become less pronounced
3[a]	11.6	Talar dome shifts posteriorly; posterior process recedes
4	7.0	Talar head shifts anteriorly
5	5.3	Medial talar neck becomes less prominent
6	4.6	Talar dome width increases
7	3.0	Posterior subtalar facet narrows
8	2.4	Posterior process prominence decreases
9	2.0	Medial talar trochlear facets become less pronounced

[a]A mode with a least 1 significant group difference.

head and neck angulating more superior-medially in individuals with CMT than in healthy controls. Significant differences in the TNOA were observed when comparing CMT1 and CMT2 types to healthy controls, supporting the hypothesis that both CMT types would have a more medial talar neck (Figure 6). These differences highlight the complexity of this disease and could have substantial implications for tailoring treatment strategies.

The flattening of the talar dome could lead to altered joint kinematics, particularly affecting dorsiflexion and plantarflexion of the tibiotalar joint. This may necessitate compensatory adjustments in adjacent joints or soft tissues, potentially increasing the risk of stress-related injuries and arthritic degeneration of the ankle joint. The superior-medial angulation of the talar head and neck observed in the CMT groups suggests further potential biomechanical and clinical consequences, including altered subtalar and talonavicular joint mechanics, variation in the locking mechanisms of the transverse tarsal joint, impacted overall gait and stability, and distorted radiographic measurements due to morphology. These changes might also predispose patients to degenerative alterations in various joints. In the CMT groups, the medial shift of the talar head would generally contribute to increased varus, internal rotation, and adduction at the subtalar and talonavicular joints, potentially exacerbating the cavovarus deformity.[18] This could result in a more rigid foot structure, impairing shock absorption and necessitating compensatory gait adaptations.[1]

These morphology variations may underscore the need to include bony realignment procedures in addition to soft tissue reconstructions when surgically treating cavovarus deformity in CMT patients. For example, the medial deviation of the talar neck in CMT patients may highlight the potential of surgical correction correcting the varus and adductus deformity of the foot.

The current literature within the 3D analysis of the foot and ankle bones in individuals with CMT has primarily focused overall alignment and measurements of the bones. Specifically,

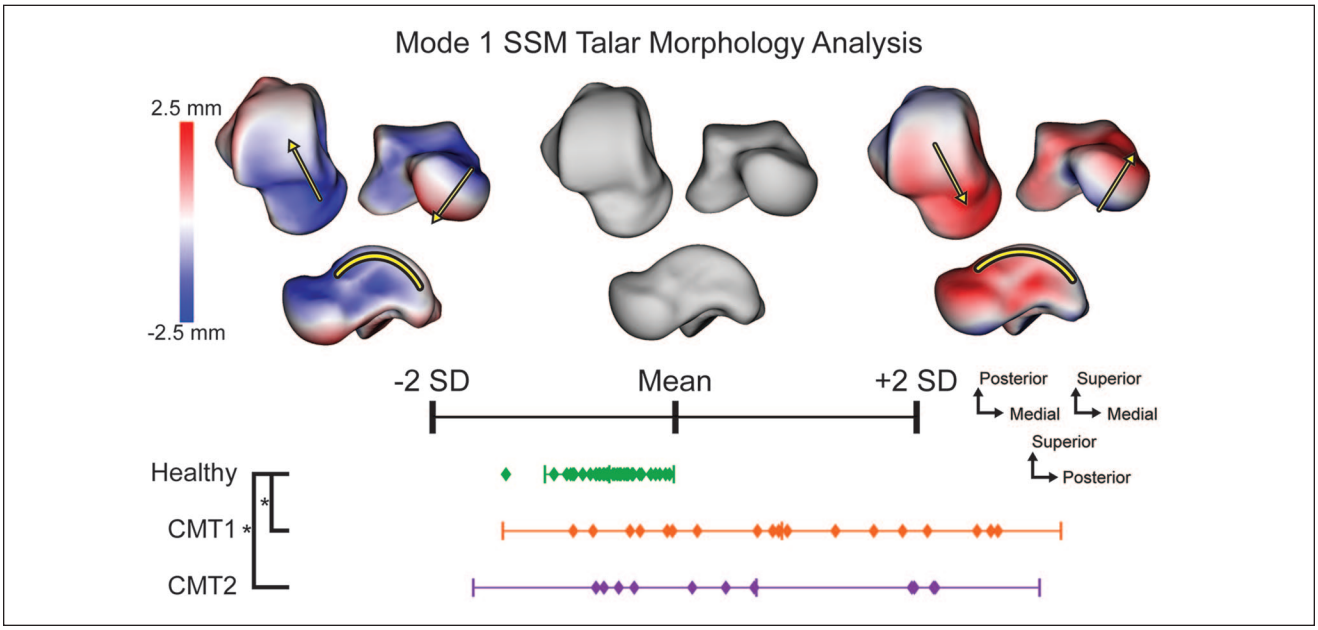

Figure 2. Mean and ±2 SDs of the first mode of variation with arrows highlighting substantial morphology changes. Normalized shape scores are plotted for each group on the same scale. The asterisks symbolize significant differences between groups.

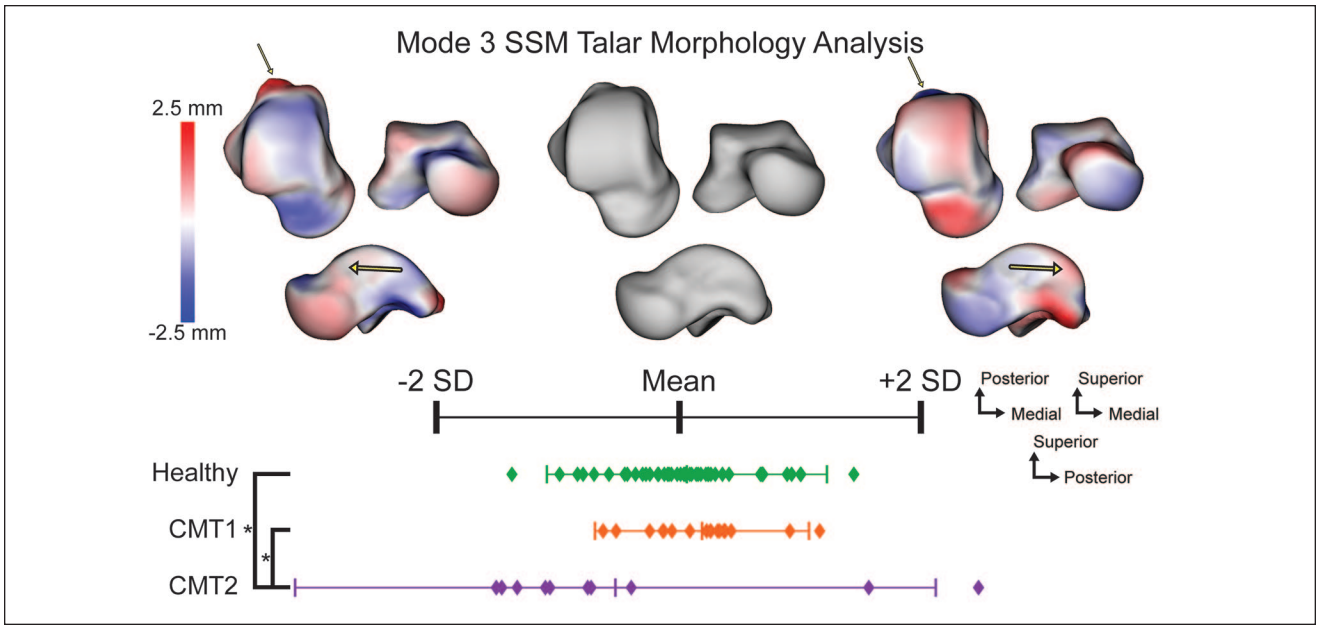

Figure 3. Mean and ±2 SDs of the third mode of variation, with arrows highlighting substantial morphology changes. Normalized shape scores are plotted for each group on the same scale. The asterisks symbolize significant differences between groups.

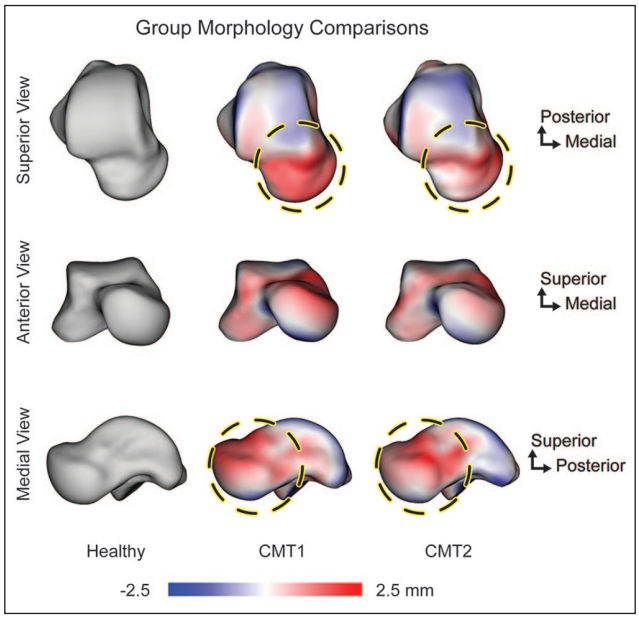

Figure 4. Morphology surface differences of the CMT1 and CMT2 groups compared with the healthy mean shape. Dashed circles are used to highlight regions of substantial morphologic variations.

Bernasconi et al[4] identified WBCT measurements, including foot and ankle offset (FAO), in cavovarus CMT patients and compared them to idiopathic cavovarus individuals focusing on inter-bone clinical relationships. Similarly, An et al[2] studied the inter-bone relationships between patients with CMT and healthy controls to find multiplanar variations of the diseased foot. Additionally, Song et al[20] identified bony measurements that show significant changes in individuals with CMT postoperatively. Although FAO is a valuable clinical measure of overall foot alignment, this study specifically focused on intra-bone morphologic changes in the talus to provide complementary insights into the biomechanical challenges faced by individuals with CMT. Although these previous studies have enhanced our understanding of foot and ankle mechanics in CMT, research on the talar bone's specific morphologic variations remains limited.

Our study does, however, draw notable parallels with the work of Michalski et al,[11] which stands out because of its similar methodological approach and patient population. Their study used finite mesh analysis and reported findings that align closely with ours, particularly regarding the underdevelopment, or flattening, of the talar dome and altered angulation of the talar neck in the CMT group. Our study expands on Michalski et al's indicating talar morphologic differences when comparing healthy controls to CMT1 and CMT2.

The study encounters certain limitations that should be acknowledged and can guide future research. One notable limitation is the relatively small sample size, particularly for the CMT2 type, which could potentially impact the interpretation and generalizability of our findings. However, as noted previously, the rarity of CMT in the general population restricts the feasibility of large-scale 3D analyses, as seen in similar studies on comparable populations.[11,12,16,20] Additionally, we include Cohen *d* to statistically determine how applicable our findings would be on a larger population.

Table 2. Mean, SD, and *P* Values of the Talar Neck Offset Angle (TNOA) for All Groups.

Group	TNOA, degrees, Mean ± SD	*P* Value
Healthy	26.85 ± 2.03	-
CMT1	28.22 ± 2.05	-
CMT2	29.60 ± 3.31	-
Group comparisons		
Healthy vs CMT1	-	0.0201[a]
Healthy vs CMT2	-	0.0010 [a]
CMT1 vs CMT2	-	0.1742

Abbreviation: CMT, Charcot-Marie-Tooth disease.
[a]Statistical significance.

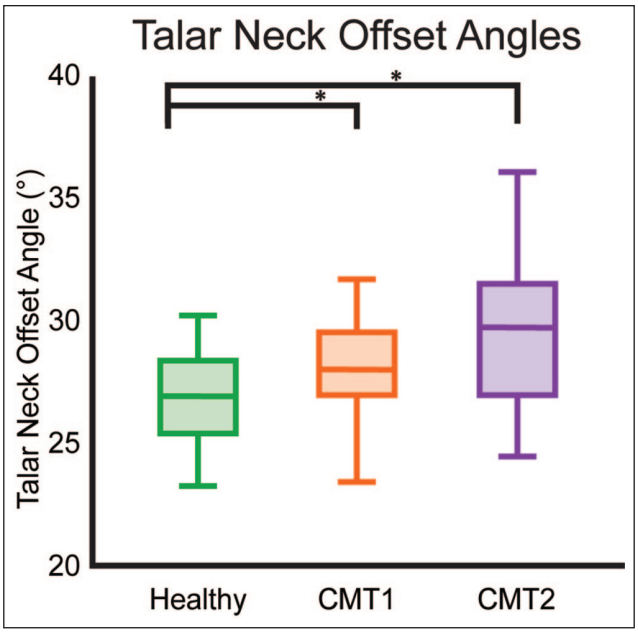

Figure 5. Box and whisker plot highlighting differences of talar neck offset angle (TNOA) measurement between groups. The asterisks symbolize significant differences between groups.

Additionally, our assumptions about functional joint interactions are inherently limited. Given the complex nature of cavovarus deformity and CMT, understanding the disease through the lens of single bone analysis provides only a partial assessment. Finally, because CMT frequently presents in adolescence, bony morphology changes may be different in individuals with symptoms before skeletal maturity than in those who did not develop symptoms until later in life, and in this study the average age at diagnosis was 36.5 years.

Conclusion

In conclusion, our study identifies specific talar morphologic changes associated with cavovarus foot deformity in CMT1 and 2, including a flattened talar dome and talar neck medial angulation. These findings highlight potential considerations for operative approaches and orthotic designs tailored to the unique challenges posed the 2 common genetic subtypes of CMT. Although further studies incorporating other foot bones and overall alignment are needed, this work may provide a foundation for refining treatment strategies to improve outcomes for individuals with CMT-related foot deformities.

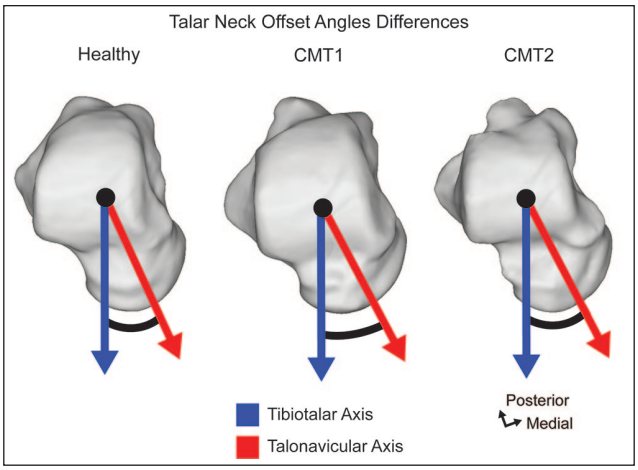

Figure 6. Representative patients' tali with anterior-posterior axes along the talar body and the talar head, highlighting the angle differences between the healthy, CMT1, and CMT2 groups.

Ethical Approval

This study was approved by the institutional review board of our affiliate institution (IRB00154634). An opt-out statement regarding the application of medical data was published on our institute's website. This study was performed under the principles of the World Medical Association Declarations of Helsinki.

Declaration of Conflicting Interests

The author(s) declared the following potential conflicts of interest with respect to the research, authorship, and/or publication of this article: Cesar de Cesar Netto, MD, PhD, reports grants/contracts: University of Iowa Department of Orthopaedics and Rehabilitation Seed Grant, Arthritis Foundation Grant, Paragon 28 Grant, AOFAS; royalties: Paragon 28, Artelon, Nextremity Solutions, Zimmer Biomet, and Medartis; Consulting Fees: Paragon 28, Zimmer Biomet, Stryker, Ossio, Artelon, Medartis, and Exactech; stock: CurveBeam and Tayco Brace; and other: Medical Advisory Board Paragon 28. Amy L. Lenz, PhD, reports general disclosures as *FAI/FAO* Specialty Content Editor. Disclosure forms for all authors are available online.

Funding

The author(s) disclosed receipt of the following financial support for the research, authorship, and/or publication of this article: Funding was provided by the University of Utah VPR Seed Grant and National Institutes of Health (NIAMS, K01AR080221). Additionally,

the National Institutes of Health supported ShapeWorks development grants (NIH U24EB029011 and NIH R01AR076120).

ORCID iDs

Andrew C. Peterson, MS, https://orcid.org/0009-0000-3516-2438
Melissa R. Requist, BS, https://orcid.org/0000-0002-4520-984X
Cesar de Cesar Netto, MD, PhD, https://orcid.org/0000-0001-6037-0685
Amy L. Lenz, PhD, https://orcid.org/0000-0003-2998-0906

References

1. Abboud R, Harrold F. Biomechanics of the foot and ankle. In: Robinson A, ed. *Core Topics in Foot and Ankle Surgery*. Cambridge University Press; 2018:22-43.
2. An T, Haupt E, Michalski M, Salo J, Pfeffer G. Cavovarus with a twist: midfoot coronal and axial plane rotational deformity in Charcot-Marie-Tooth disease. *Foot Ankle Int*. 2022;43(5):676-682. doi:10.1177/10711007211064600
3. Barreto LC, Oliveira FS, Nunes PS, et al. Epidemiologic study of Charcot-Marie-Tooth disease: a systematic review. *Neuroepidemiology*. 2016;46(3):157-165. doi:10.1159/000443706
4. Bernasconi A, Cooper L, Lyle S, et al. Pes cavovarus in Charcot-Marie-Tooth compared to the idiopathic cavovarus foot: a preliminary weightbearing CT analysis. *Foot Ankle Surg*. 2021;27(2):186-195. doi:10.1016/j.fas.2020.04.004
5. Cates JE, Elhabian SY, Whitaker RT. ShapeWorks: particle-based shape correspondence and visualization software. In: *Statistical Shape and Deformation Analysis*. Elsevier; 2017:257–298.
6. Han Q, Liu Y, Chang F, Chen B, Zhong L, Wang J. Measurement of talar morphology in northeast Chinese population based on three-dimensional computed tomography. *Medicine (Baltimore)*. 2019;98(37):e17142. doi:10.1097/md.0000000000017142
7. Holmes JR, Hansen ST Jr. Foot and ankle manifestations of Charcot-Marie-Tooth disease. *Foot Ankle*. 1993;14(8):476-486. doi:10.1177/107110079301400809
8. Horn JL. A rationale and test for the number of factors in factor analysis. *Psychometrika*. 1965;30:179-185. doi:10.1007/bf02289447
9. Laurá M, Singh D, Ramdharry G, et al. Prevalence and orthopedic management of foot and ankle deformities in Charcot-Marie-Tooth disease. *Muscle Nerve*. 2018;57(2):255-259. doi:10.1002/mus.25724.
10. Ledesma RD, Valero-Mora P. Determining the number of factors to retain in EFA: an easy-to-use computer program for carrying out parallel analysis. *Pract Assess Res Eval*. 2007;12(1):2. doi:10.7275/wjnc-nm63
11. Michalski MP, An TW, Haupt ET, Yeshoua B, Salo J, Pfeffer G. Abnormal bone morphology in Charcot-Marie-Tooth disease. *Foot Ankle Int*. 2022;43(4):576-581. doi:10.1177/10711007211055460
12. Michalski MP, Blough CL, Song JH, Pfeffer GB. Méary's angle decoded: 3D analysis of first ray plantarflexion deformity in Charcot-Marie-Tooth disease. *Foot Ankle Surg*. 2024;S1268-7731(24):00182-6. doi:10.1016/j.fas.2024.08.003
13. Okamoto Y, Takashima H. The current state of Charcot-Marie-Tooth disease treatment. *Genes (Basel)*. 2023;14(7):1391. doi:10.3390/genes14071391
14. Parr WC, Chatterjee HJ, Soligo C. Calculating the axes of rotation for the subtalar and talocrural joints using 3D bone reconstructions. *J Biomech*. 2012;45(6):1103-1107. doi:10.1016/j.jbiomech.2012.01.011
15. Peterson AC, Kruger KM, Lenz AL. Automatic anatomical foot and ankle coordinate toolbox. *Front Bioeng Biotechnol*. 2023;11:1255464. doi:10.3389/fbioe.2023.1255464
16. Ranjit S, Sangoi D, Cullen N, Patel S, Welck M, Malhotra K. Assessing the coronal plane deformity in Charcot Marie Tooth Cavovarus feet using automated 3D measurements. *Foot Ankle Surg*. 2023;29(7):511-517. doi:10.1016/j.fas.2023.02.013
17. Saporta AS, Sottile SL, Miller LJ, Feely SM, Siskind CE, Shy ME. Charcot-Marie-Tooth disease subtypes and genetic testing strategies. *Ann Neurol*. 2011;69(1):22-33. doi:10.1002/ana.22166
18. Sarrafian SK. Biomechanics of the subtalar joint complex. *Clin Orthop Relat Res*. 1993;290:17-26.
19. Shy ME, Chen L, Swan ER, et al. Neuropathy progression in Charcot-Marie-Tooth disease type 1A. *Neurology*. 2008;70(5):378-383. doi:10.1212/01.wnl.0000297553.36441.ce
20. Song JH, Michalski MP, Pfeffer GB. 3D analysis of joint-sparing Charcot-Marie-Tooth surgery effect on initial standing foot alignment. *Foot Ankle Int*. 2024;45(6):601-611. doi:10.1177/10711007241232976
21. Theadom A, Roxburgh R, MacAulay E, et al. Prevalence of Charcot-Marie-Tooth disease across the lifespan: a population-based epidemiological study. *BMJ Open*. 2019;9(6):e029240. doi:10.1136/bmjopen-2019-029240
22. Wilm J.. *Iterative Closest Point*. 1.14.0.0 ed. MATLAB Central File Exchange; 2023.